Rotorcraft Design and Analysis

Soufiane El Omari

Design of a rotor-craft by optimization

The preliminary sizing of a rotor-craft allows for estimation of basic geometry and performance parameters starting from mission requirements. We define basic requirements on the type and class of the target helicopter. In this report, the sizing and optimization procedure for a light, single engine civil helicopter to be used for two missions: mission 1 related to rescue, and mission 2 related to crop spraying.

The related missions for this helicopter are shown in Table 1, the first mission gives range requirements for carrying crew and payload, while the second mission covers the endurance requirements.

Table 1: Mission profiles

Mission 1	Requirement	Mission 2	Requirement
Crew weight, kg	170	Crew weight, kg	85
Payload, kg	360	Payload, kg	190
Cruise speed, m/s	55	Loiter speed, m/s	50
Range, km	600	Endurance, h	3.5
Air density, kg/m^3	1.1116	Air density, kg/m^3	1.225

Along side these requirements we define basic helicopter data to use in the optimization function.

no. of m.r. blades : 3
hinge offset e [non-dim.] : 0.05
fuselage diameter [m] : 2
no. of engines : 1
specific fuel consumption [kg.hr/hp] : 0.23
no. of retractable landing gear wheels : 3
no. of t.r. blades : 2
Mach no. at m.r. tip : 0.63
horizontal stabilizer surface [m^2] : 2
Cl_α horizontal stabilizer [1/rad] : 4.6
Hover weighing parameter K_1 : 1
Forward flight weighing parameter K_2 : 13

With the preliminary data, we minimize the following function to obtain a guess for the

geometry and properties of the helicopter:

$$min[K_1(P_{mr_{hov}}(x) + P_{tr_{hov}}(x)) + K_2(P_{mr_{fwd-cruise}}(x))]$$

where **x** is a vector containing helicopter parameters used to compute the power, P is the power, K_1 and K_2 are the weighing parameteres for hover and forward flight respectively. Using Blade element theory we compute the power required by the main and tail rotors in hover, while only the main rotor power is computed for cruising flight. A guess of the initial conditions is computed from momentum theory and FMR.

Let us compare the output of the weight parameters for different forward flight parameter K_2, with $K_1 = 1$. this data is found in Table 2.

Table 2: Weight comparison for different K_2

Weight parameter	K_2= 0	K_2=6	K_2=13
MTOW, kg	1571.0625	1918.3755	1972.9437
mOW, kg	1040.33	1146.3833	1171.4593
TOW 1, kg	1562.716	1706.4253	1736.8006
Fuel 1, kg	162.3859	200.042	205.3413
TOW 2, kg	1571.0625	1918.3755	1972.9437
Fuel 2, kg	425.7324	666.9922	696.4844

Weight comparison shows minimal difference between the hover + fwd optimizations. The weight difference between the two missions is around 200 kg. However, There is a slight decrease in fuselage length for K_2=13 at 7.25m.

The main-rotor sizing parameter for the chosen configurations are shown in Table 3.

Table 3: Rotor Comparison for different K_2

Main rotor parameters	K_2=0	K_2=6	K_2=13
R, m	4.4102	4.4102	4.4102
ω, rad/s	48.5696	44.5532	43.6825
V_tip, m/s	214.2	196.4871	192.647
Solidity	0.040724	0.091383	0.10195
Root chord, m	0.36621	0.5542	0.52408
Mean chord, m	0.18808	0.42204	0.47083
Tip chord, m	0.1287	0.37485	0.45308
constant chord %	0	4.9811	0.0037146
Twist angle, deg	0	-2.4117	-2.4507

When comparing blade properties, we notice an increase in solidity with increasing K_2. The blade radius and tip speed are comparable. However, the blade geometry is better in the case of "hov+fwd" optimization.

The rotor performance in hover is characterized by the data shown in Table 4. We notice an increase in thrust and power required when optimizing for hover and forward flight. The difference in disk loading across the configuration prevents us from using the FM as performance indicator.

Table 4: Hover Comparison for different K_2

Hover parameters	$K_2 = 0$	$K_2 = 6$	$K_2 = 13$
T, N	15412.1228	18819.2637	19354.5773
P, KW	207.3697	283.5678	297.4505
θ_0, deg	11.4592	11.4592	11.4592
PL, N/KW	74.322	66.366	65.0682
DL, N/m^2	252.2338	307.9948	316.7557
FM	0.75411	0.74411	0.73986
c_t/σ	0.1102	0.071264	0.068341

Lastly we compare the performance in forward flight. It is clear from Table 5 data that the parameters are comparable in the case of $K_2 > 1$, due to the similarity in weight results from the optimization process.

Table 5: Forward flight Comparison for different K_2

For. Flight parameters	$K_2 = 0$	$K_2 = 6$	$K_2 = 13$
T, N	15930.3211	19351.2264	19885.364
P, KW	332.012	281.5442	282.4028
θ_0, deg	12.1841	9.3842	9.2476
a_1, deg	6.5135	5.0758	5.0414
B_1, deg	6.5135	7.4044	7.2776
γ, deg	3.1255	3.3591	3.3677
α_D, deg	6.5024	5.6877	5.6039

Trim of the helicopter

Triming a helicopter is an exersice of finding the correct forces and moment with equilibrium about the hub center. Using the force method, we can solve a linear set of 14 equations in 16 unknowns, by assigning either flight conditions or controls.

The helicopter is tested for trim in longitudinal condition using the output of the optimization script. Similarly to the previous assignment, we use a force method assigning the flight conditions and finding the correct forces and moments to trim the aircraft in forward flight.

To solve for the rest of the variables, a Newton method is proposed.

$$\mathbf{x_{n+1}} = \mathbf{x_n} - \mathbf{J}(\mathbf{x_n})^{-1}\mathbf{F}(\mathbf{x_n})$$

Where $\mathbf{x}$ is the vector of unknowns, $\mathbf{F}(\mathbf{x_n})$ is a vector of non-linear equations, and $\mathbf{J}(\mathbf{x_n})$ is the jacobian of F. The problem converges when we reach an error lower than the assigned tolerance of $\varepsilon = 10^{-2}$

For the purpose of computing the Jacobian matrix, we create a function of all the equations and unknowns in symbolic form, then use *jacobian(F,x)* in matlab to find the partial derivatives.

The sweep analysis for the helicopter is shown in the figures below, where the change of thrust and pitch angle required with respect to the weighing parameter K2 are shown in Figure 11. The trend of controls are shown in Figure 2.

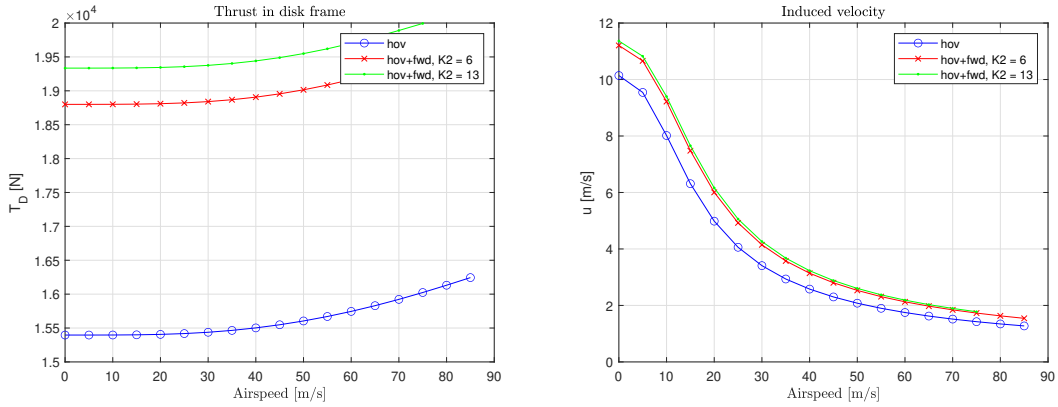

Figure 1: Thrust and Induced velocity with respect to V_∞ for different optimizations

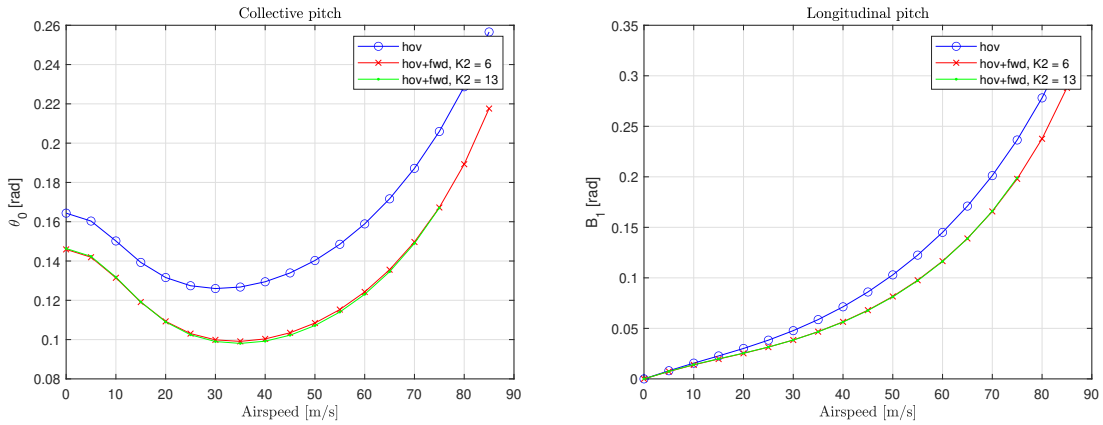

Figure 2: Controls with respect to V_∞ for different optimizations

When comparing the trim data, we notice that an increase in thrust comes with a decrease in pitch required for the "hov+fwd" optimizations. However the Induced velocity is higher. Assessment of the previous data shows that $K_2 = 13$ has slightly better efficiency and geometry, and will be chosen for the upcoming analysis.

Computation of the center of gravity

To find the approximate center of gravity position for the helicopter, the following sketch is proposed (Figure 13). The light helicopter features two rows with the crew in front and the passengers at the back. The rotor is located at 55% of the fuselage length, with the fuel and equipment compartment towards the end.

Figure 3: Sketch of the helicopter

The position of the CG is computed using estimates of the position of the different stations. Figure 10 shows the layout of the helicopter. Table 6 shows the weight distribution and position of the helicopter CG.

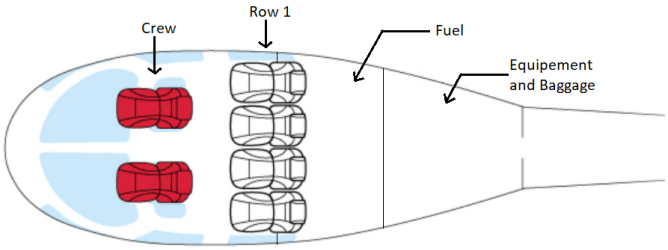

Figure 4: Helicopter layout for Mission 1

Table 6: Computation of empty helicopter CG

Component	Weight, kg	Station, m	Moment, Nm
Blades (m.r)	110.75	3.76	417.48
Head (m.r)	51.08	0.86	44.43
Tail rotor	4.48	10.14	45.53
Fuselage	249.45	3.98	994.56
Landing gear	61.85	4.71	291.46
Drive system	111.78	3.77	421.35
Fuel system	13.31	3.91	52.10
Installed motor	76.12	3.62	275.91
Flight controls	89.19	0.72	64.65
Avionics	233.40	5.07	1184.35
Total weight		1001.45kg	
CG position		3.78 m	

An estimate of the envelope of TOW w.r.t the longitudinal center of mass location is shown in Figure 5. The center of mass position is given with respect to the fuselage length, starting from the front. As seen from the previous sketch the lumped position of fuel is behind row1, with the baggage at the back.

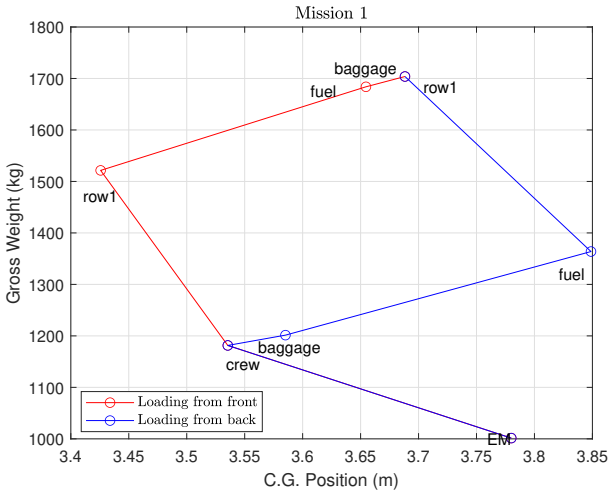

Figure 5: Helicopter layout for Mission 1

We run the trim procedure for different TOW configurations and compare their performances. The configurations include the MTOW for missions 1 as well as loading of crew, fuel, and passengers separately. Figure 16 displays the trend of different trim parameters at the chosen configurations.

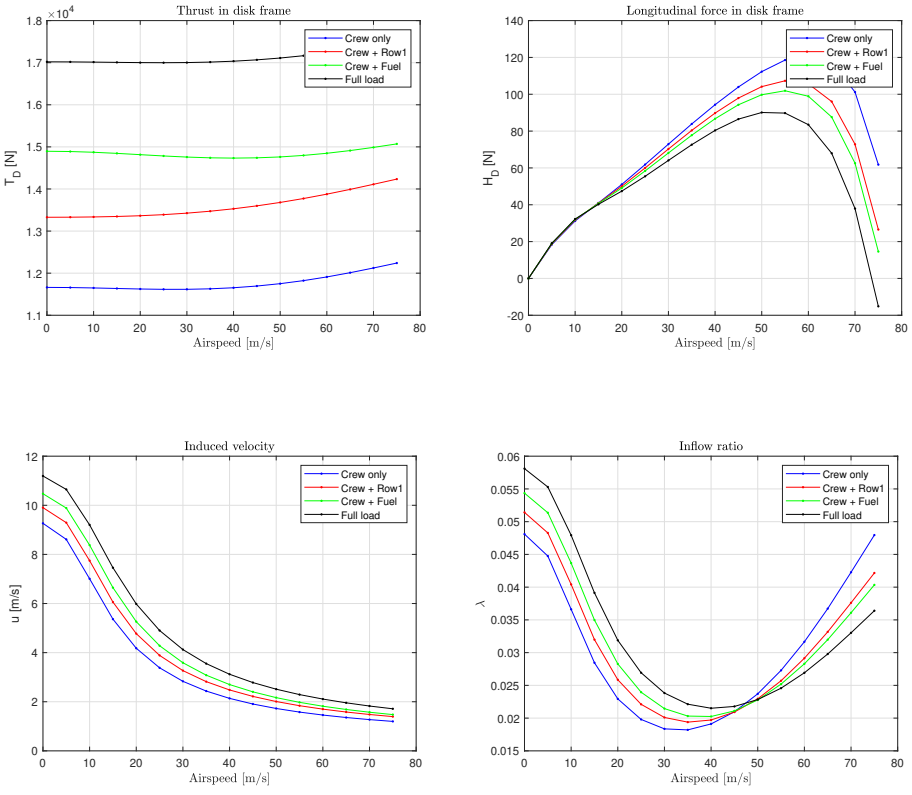

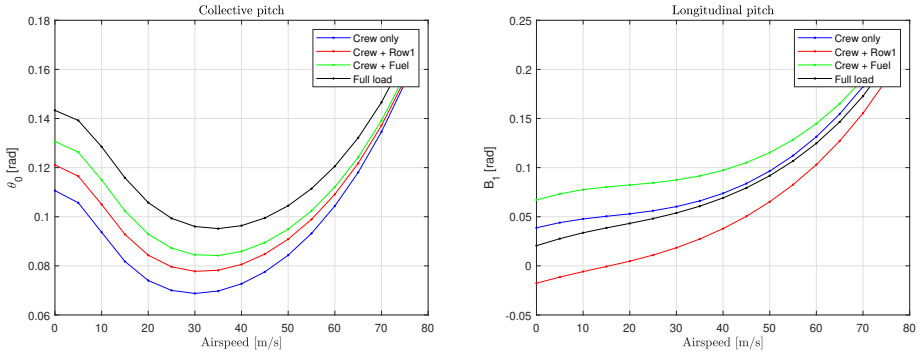

Figure 6: Trim parameters with respect to V_∞ for different loading configurations

It is clear that with an increase in weight the thrust required jumps up, this trend is also seen in the longitudinal force H_D. There is also a change in the control angle required for the trim. The inflow ratio λ shows an interesting trend where it becomes higher close to 50 m/s, which is around the cruising speed specified for Mission 1.

Blade Flexibility Analysis

The blade rotation modes will be analyzed for a the helicopter using the blade characteristics found during the sizing campaign. The blades are tested from 0 to 120% of the nominal rotating speed of $\omega = 43.68$ rad/sec.

The blade data are shown in Table 7.

Table 7: Rotor data

Main rotor parameters	Value
R, m	4.4102
ω, rad/s	43.6825
V_tip, m/s	192.647
Solidity	0.10195
Root chord, m	0.52408
Mean chord, m	0.47083
Tip chord, m	0.45308
constant chord %	0.0037146
Twist angle, deg	-2.4507

We start by designing a model of the helicopter blade using FEMAP from the defined data. A finite element model of the blade is then created starting from the basic geometry, with a mesh size of 50x10.

Figure 1 shows the FEM of the blade.

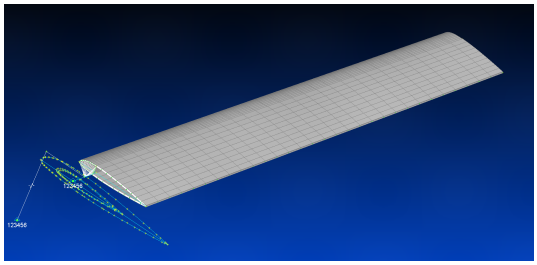

Figure 7: FEM blade model

The blade modes are tested at angular velocities from 0 to 120% of the nominal speed using NASTRAN. Figure 8 shows four rotating modes at 0%ω and Figure 9 at 80%ω.

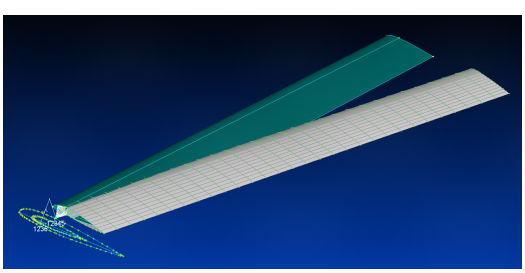

(a) First lag

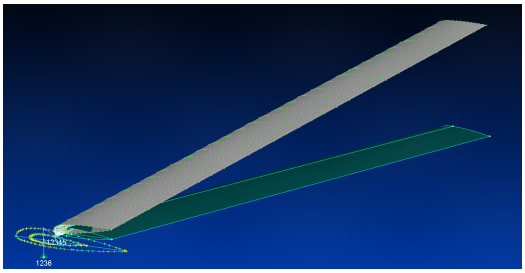

(b) First flap

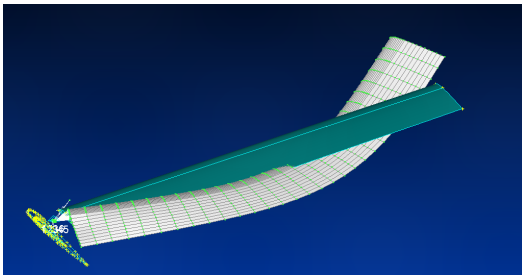

(c) Second lag

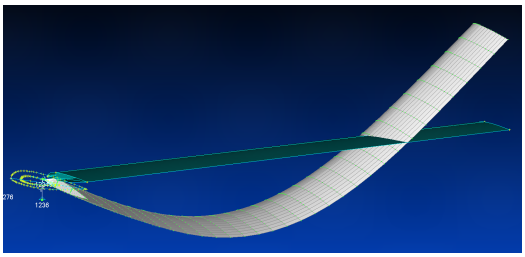

(d) Second Flap

Figure 8: Rotating modes at 0%ω

The rest of the modes data are summed up in Table 11 and Table 9 with the frequency of each mode at different nominal angular velocities.

Table 8: Mode frequencies from 0%ω to 50%ω

Mode	0% Ω	10% Ω	20% Ω	50% Ω
First Lag	2.19E-04	0.145779	0.296442	1.054925
First Flap	0.0974085	0.689726	1.365222	3.478736
Second Flap	12.06973	12.18836	12.53359	14.88341
First Torsion	34.45668	34.49717	34.59794	37.07057

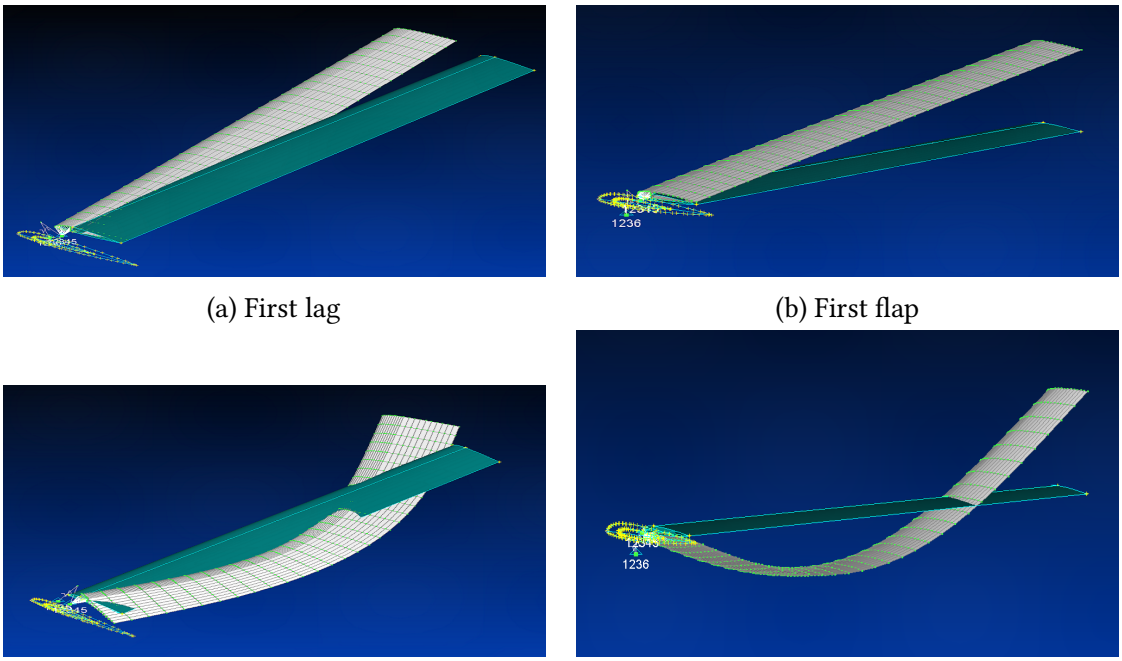

(a) First lag

(b) First flap

(c) Second lag

(d) Second flap

Figure 9: Rotating modes at 80%ω

Table 9: Mode frequencies from 50%ω to 120%ω

Mode	80% Ω	100% Ω	110% Ω	120% Ω
First Lag	1.680695	2.09222	2.295822	2.497884
First Flap	5.556374	6.93929	7.629413	8.319045
Second Flap	18.35808	21.03043	22.43258	23.86833
First Torsion	39.61792	41.23466	42.01287	42.79594

We notice a steady increase in frequency of the modes with the increase in angular velocity.

Plotting the frequencies with respect to angular velocities gives us the fanplot shown in Figure 10. It is necessary that the blade does not present eigen-frequencies close the harmonics at 1/rev to 8/rev.

With close inspection of the result of the fanplot below, we notice that modes 3 and 4 cross the harmonics of the blade at 3/rev and 6/rev respectively. It is necessary to change the mass distribution or stiffness to update the frequencies and avoid instability. It is also possible to position the lumped mass correctly along the span to obtain better results.

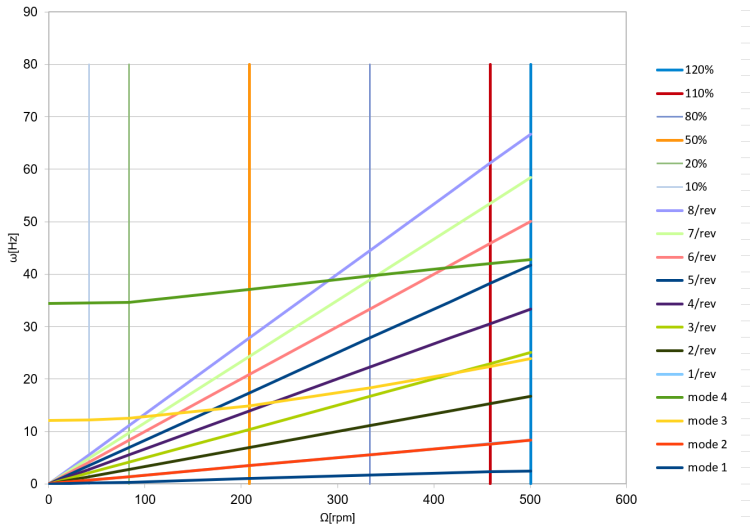

Figure 10: Fanplot

Ground resonance analysis

Deutsch criterion

Ground resonance is a severe stability issue stemming from the coupling of the hub and lag motions. The blade lead/lag creates a resonance when the frequency is below 1/rev as is the case for articulated and soft-in-plane rotors. Depending on the angular velocity of the rotor, the resonance is characterized by an oscillatory motion that can lead to serious damage on the landing gear and air frame. The previously designed light weight single engine helicopter will be tested for ground resonance instability over a range of velocities from 40% to 120% of the maximum operating angular velocity, with various loading configurations. The main helicopter data is summarized below.

no. of m.r. blades: 3
main rotor radius [m]: 4.41
main rotor mass [kg]: 110.75
hinge offset e [non-dim.]: 0.05
fuselage diameter [m]: 2
no. of engines: 1
mOW [kg]: 1171.45
TOW1 [kg]: 1736.80
TOW2 [kg]: 1972.94

The study of resonance requires analysing the coupling of the lead/lag dynamics with the rotor. By considering the blade static moment S_ζ to be small, we can derive an equation for the stability boundary exactly at the resonance, which is most critical for the system. The minimum required lag damping to avoid the instability at peak resonance is given by the Deutsch criterion. This criterion defines a restriction on the resonance of low-frequency modes and provides an approximate of the stability region in soft-in-plane motion:

$$\frac{C_x C_\zeta}{\omega_x^2} = \frac{N}{4} \frac{1 - \nu_\zeta}{\nu_\zeta} S_\zeta^2$$

For this purpose, we define the symmetric inertia tensor, and basic geometric parameters of the landing gear used in the helicopter.

$$I_{cg} = \begin{bmatrix} I_x & 0 & 0 \\ 0 & I_y & 0 \\ 0 & 0 & I_z \end{bmatrix}$$

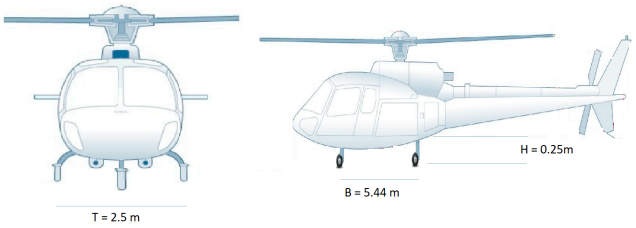

Figure 11: Geometry of the Landing Gear

Analysis for articulated and soft in plane rotors

The ground resonnance analysis is performed for an articulated rotor. Table 10 shows the output data for different TOW values.

Table 10: Deutsch criterion of different loading configurations

Output	mOW	Mission 1	Mission 2
Lag motion nat. freq.	0.28098/rev	0.28098/rev	0.28098/rev
Soft-in-plane rotor	yes	yes	yes
Deutsch Criterion	168.27 Nms/rad	249.48 Nms/rad	283.41 Nms/rad

It is clear that with increasing loading the required lag damping is higher. Figures 12 and 13 show the trend of the real part of the natural frequency for the loading configurations (Deutsch criterion satisfied).

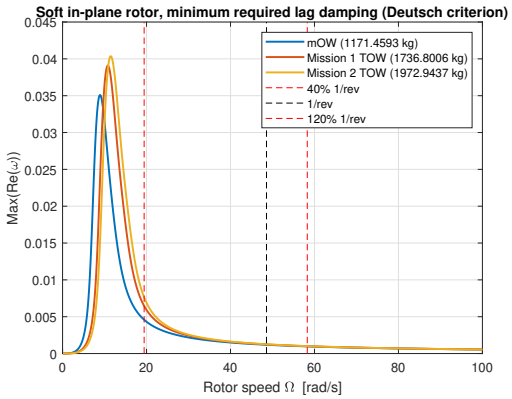

Figure 12: Undamped Solution

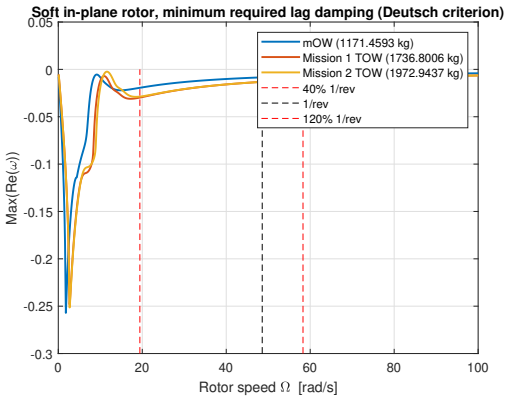

Figure 13: Result with C > C_D

Ground resonance is not possible for stiff-in-plane rotors, which are characterized by a lag frequency $\upsilon_\zeta > 1/\text{rev}$. This happens exactly at a lag spring stiffness of $K = 445800 Nm/rad$.

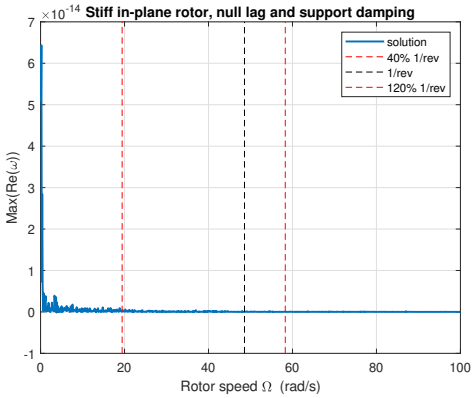

Figure 14: Undamped Solution

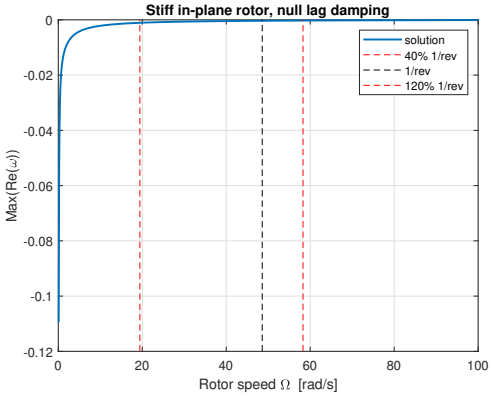

Figure 15: Stiff-in-plane Solution

The Deutsch criterion is always satisfied, the system is neutrally stable.

Model analysis using ADAMS

Stability analysis

The helicotper will be verified using high-fidelity simulation software ADAMS. To start the analysis, a model of the aircraft is constructed with the input data found in Table 11.

Table 11: Helicopter Data

Parameter	Value
Fuselage mass, kg	249.45
Shaft mass, kg	10
Fuselage Ixx, kg.m^2	2508.18
Fuselage Iyy, kg.m^2	12566.54
Fuselage Izz, kg.m^2	12004.98
Blade mass, kg	110.75
Blade Ixx, kg.m^2	200
Blade Iyy, kg.m^2	200
Blade Izz, kg.m^2	2
Rotational velocity, rad/s	48.56

The response of the system consists of 9 modes, 1 for each degree of freedom totaling 6, and 1 for each main rotor blade. A sketch of the helicopter model is shown in Figure 16.

The stability of the helicopter is assessed in static (left) and dynamic case (right). The results of the analysis are shown in Figure 17.

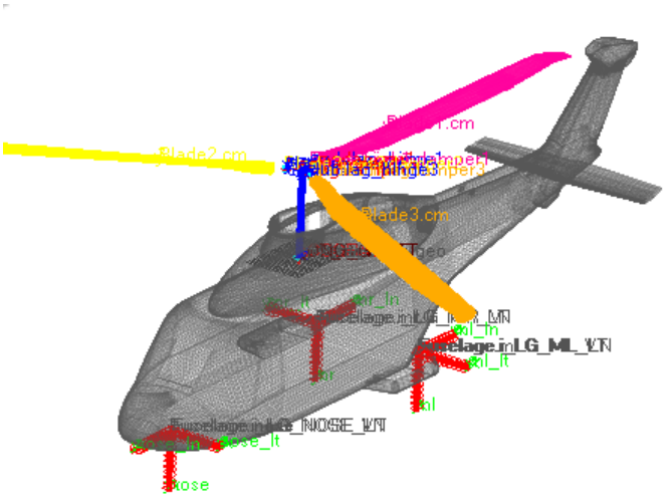

Figure 16: Helicopter Model

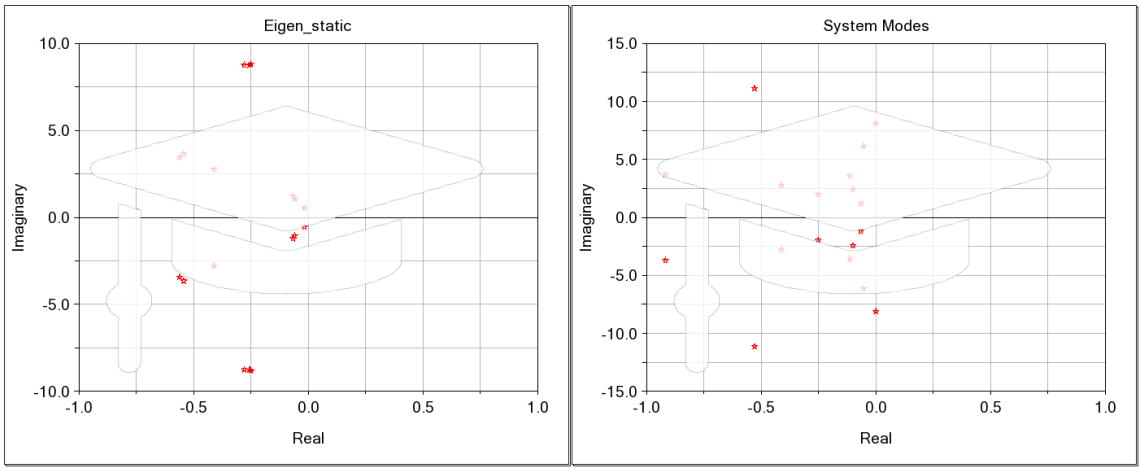

Figure 17: Eigenanalysis of the System

The system is stable when tested from start to maximum angular velocity.

Figure 18 shows the change of force in the lag dampers and hub with increasing angular velocity. The torque is displayed in Figure 19 where we see a higher oscillation of the hub when reaching maximum velocity. The effect of the lag motion on the center of mass is shown in Figure 20.

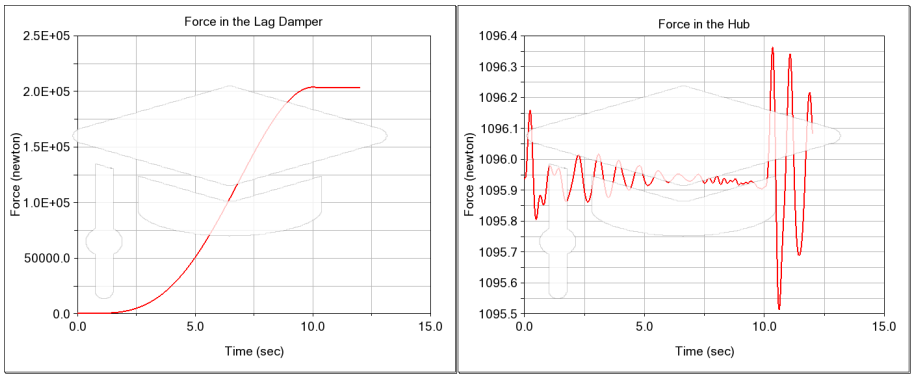

Figure 18: Force in the Damper and Hub

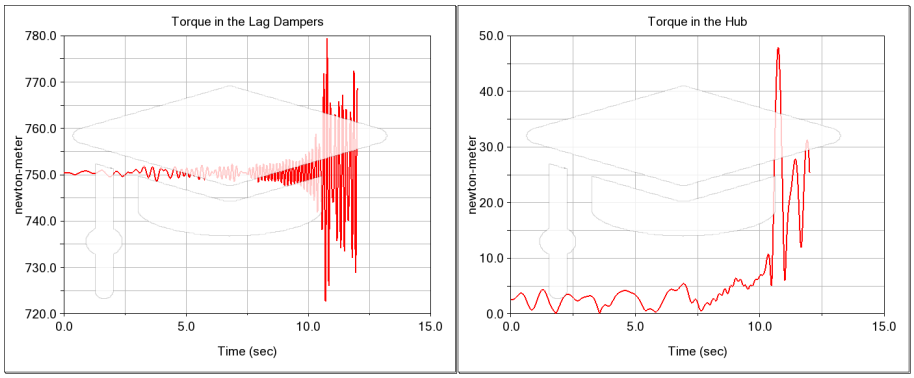

Figure 19: Torque in the Damper and Hub

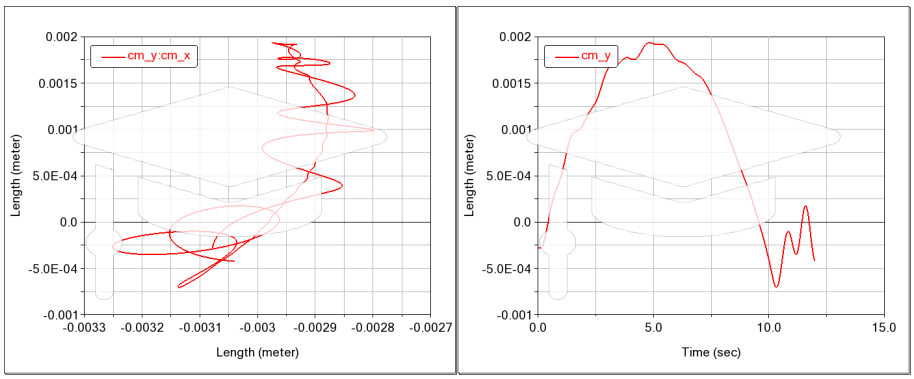

Figure 20: Position of the CM in the y Direction

We notice a change in the position of the center of mass due to the lag motion. Plotting the position in the XY-plane allows us to visualize the movement of the center of mass as seen from above.

Gust response

We introduce a lateral and longitudinal gust to the model and study the response of the system. The gusts are given by step functions as seen in Figure 21.

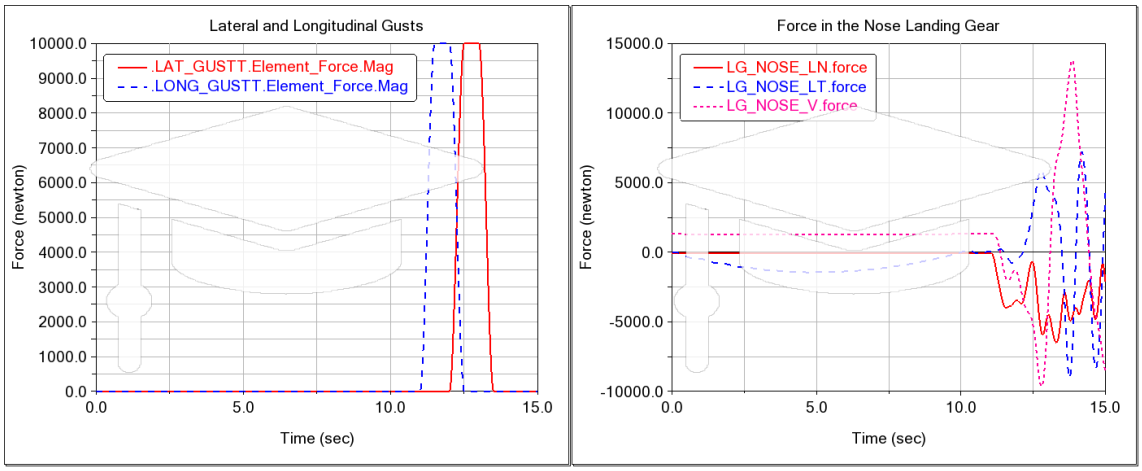

Figure 21: Gust Profile and Response

The gusts are set to happen around the same time, to excite the system in a significant way. The gusts affect the nose landing gear, introducing some forces in every direction. There is also an effect of the gust on the center of mass of the helicopter, which is more pronounced for the lateral gust.

Parametric analysis

A parametric analysis of the damping in lag motion shows the minimum value of damping at which the relative angular velocity of the lag motion doesn't change. From Figure 22 we see find the value of the damping close to $110 Nm/s$.

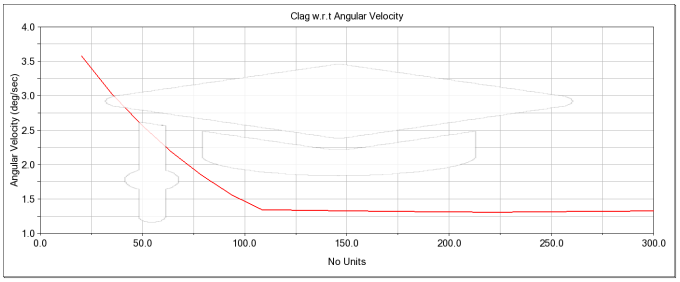

Figure 22: Clag Trend w.r.t Relative Angular Velocity

A failure of the lag damper will create an impulse characterized by a peak in torque. The effects of this impulse can be studied using an ADAM script. An impulse is performed at 11.5 seconds after start and is coupled with an engine failure. The effect of the impulse on the lag damper is shown in Figure 23. The failure of the engine is displayed in Figure 24.

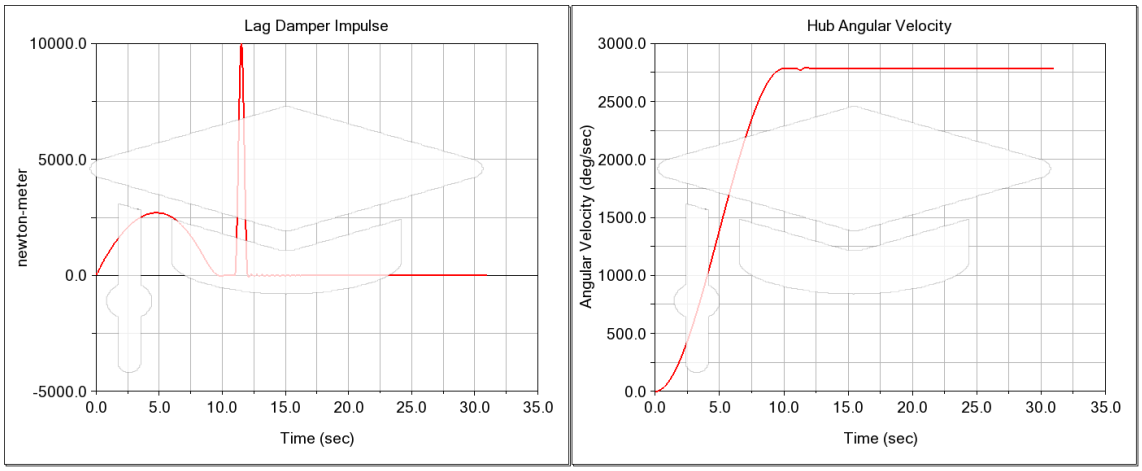

Figure 23: Impulse in the lag damper and effect on angular velocity

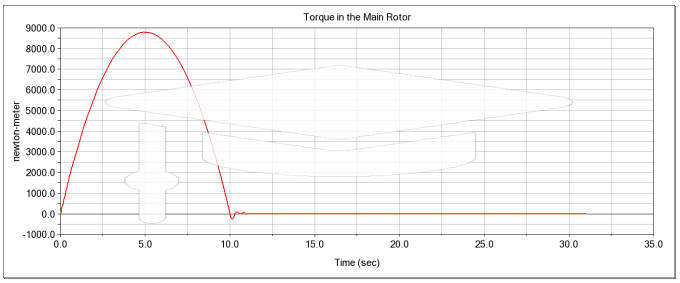

Figure 24: Torque in Main Rotor due to Engine Failure

This critical condition results in an unstable behavior of the helicopter. The deformation of the rotor can be seen in Figure 25, the rest of the helicopter components experience similar effects.

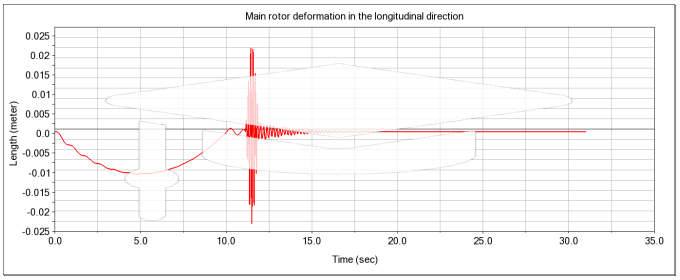

Figure 25: Main Rotor Deformation due to Engine Failure

Lastly, we can analyse the change in angular velocity for different damping and impulse values when the system is failing. Each combination is characterized by a final value of angular velocity in deg/sec.

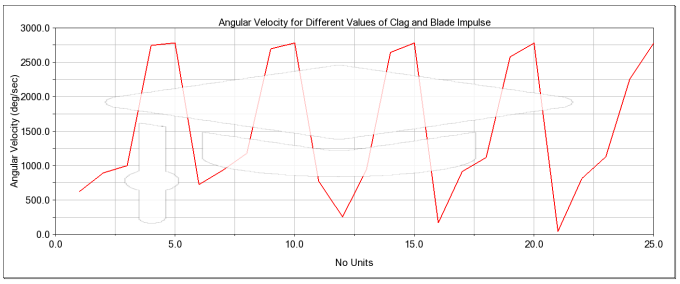

Figure 26: Final Angular Velocity at Each Run

We choose a damping of 200 Nm/s and an impulse equal to 10000N and check the effect on the angular velocity shown in the figure below.

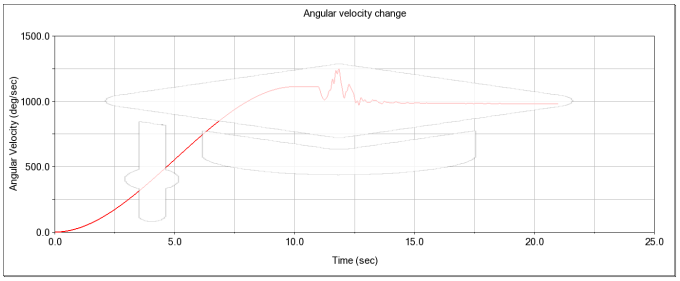

Figure 27: Angular Velocity change due to Failure